Early-Warning Signals for the Onsets of Greenland Interstadials and the Younger Dryas–Preboreal Transition

MARTIN RYPDAL

Department of Mathematics and Statistics, UiT The Arctic University of Norway, Tromsø, Norway

(Manuscript received 20 November 2015, in final form 8 February 2016)

ABSTRACT

The climate system approaches a tipping point if the prevailing climate state loses stability, making a transition to a different state possible. A result from the theory of randomly driven dynamical systems is that the reduced stability in the vicinity of a tipping point is accompanied by increasing fluctuation levels and longer correlation times (critical slowing down) and can in principle serve as early-warning signals of an upcoming tipping point. This study demonstrates that the high-frequency band of the δ^{18}O variations in the North Greenland Ice Core Project displays fluctuation levels that increase as one approaches the onset of an interstadial (warm) period. Similar results are found for the locally estimated Hurst exponent for the high-frequency fluctuations, signaling longer correlation times. The observed slowing down is found to be even stronger in the Younger Dryas, suggesting that both the Younger Dryas–Preboreal transition and the onsets of the Greenland interstadials are preceded by decreasing stability of the climate state. It is also verified that the temperature fluctuations during the stadial periods can be approximately modeled as a scale-invariant persistent noise, which can be approximated as an aggregation of processes that respond to perturbations on certain characteristic time scales. The results are consistent with the hypothesis that both the onsets of the Greenland interstadials and the Younger Dryas–Preboreal transition are caused by tipping points in dynamical processes with characteristic time scales on the order of decades and that the variability of other processes on longer time scales masks the early-warning signatures in the δ^{18}O signal.

1. Introduction

Analysis of the relative variations of the ^{18}O isotope in Greenland ice cores shows that there was a sequence of large and abrupt temperature changes during the most recent ice age. The most prominent of these changes are the transitions between the cold stadial periods and the warmer interstadial periods, during which the temperature typically increased by about 10°C within a couple of decades. The onset of the Greenland interstadials (GIs) were often followed by a slow cooling, which in some cases persisted for millennia, before there were more rapid transitions back into the stadial state. These cycles are called Dansgaard–Oeschger (DO) events (Dansgaard et al. 1984, 1993). In this paper we analyze the ice-core record from the North Greenland Ice Core Project (NGRIP) for the time period from 60 kyr before present (BP)[1] to the commencement of the Holocene, in which previous studies have identified 17 DO events (Svensson et al. 2008). The termination of the Younger Dryas (YD), the last stadial period seen in the Greenland ice cores, marks the end of the last glacial period, but this event does not define the onset of a DO cycle. However, there is little agreement in the scientific literature as to what the mechanisms for the YD were (Broecker et al. 2010), and since the YD–Preboreal transition is as abrupt as the onsets of the interstadials, it is natural to include this event in this investigation.

It is widely accepted that the onset of an interstadial period is associated with an abrupt loss of sea ice in the North Atlantic as a response to a change in the meridional overturning circulation (MOC) (Bond et al. 2013; Li et al. 2010). Positive feedback effects, such as the sea ice–albedo feedback (Curry et al. 1995) and the sea ice–insulation feedback (Manabe and Stouffer 1980), can

Denotes Open Access content.

Corresponding author address: Martin Rypdal, UiT The Arctic University of Norway, 9037 Tromsø, Norway.
E-mail: martin.rypdal@uit.no

DOI: 10.1175/JCLI-D-15-0828.1

[1] Here the present is taken to be 2000 CE.

accelerate the effect of a changing ocean circulation and cause rapid warming as a nonlinear response.

The mechanisms of the MOC variations during the last ice age and their relation to the DO events are not well understood (Broecker et al. 2010). It is believed that the MOC was subject to rapid changes in response to freshwater perturbations, but it is not clear which forcing agent is responsible for these changes. Grootes and Stuiver (1997) have reported a spectral peak in the δ^{18}O records from the Greenland Ice Core Project (GRIP) at a frequency corresponding to a period of about 1470 yr, and it has been suggested that this periodicity is produced by the de Vries/Suess and Gleissberg solar cycles (Suess 2006; Sonett 1984) (which have observed periods of 208 and 88 yr, respectively). The mechanism by which the spectral peak in the δ^{18}O records could be linked to the shorter solar cycles is the phenomenon known as ghost resonance (Balenzuela et al. 2012), and the plausibility of this explanation has been established by demonstrating that a 1470-yr periodicity in temperature can be produced from climate models if one explicitly introduces the periodicities of 208 and 88 yr in the salinity perturbations of the MOC (Braun et al. 2005). Ditlevsen et al. (2007) have pointed out that it is difficult to establish statistical significance of the 1470-yr periodicity in the ice-core data and that the DO events may be triggered randomly by noise-like fluctuations in the climate system. Other authors have suggested that the DO oscillation is linked to a limit cycle in a low-dimensional dynamical system describing the MOC (Sakai and Peltier 1999).

Whether the DO cycles are noise induced is of course not a closed-ended question, and the answer depends to some extent on the modeling framework. Temperature variations in general have unpredictable (or random) components on all the relevant time scales, and the high-frequency temperature fluctuations in Greenland during the last glacial period had a magnitude only a few times smaller than the typical temperature difference between the stadial and interstadial states. This suggests that random fluctuations may be important triggers of the DO events, but it does not exclude the possibility that there are slow changes in the climate conditions, perhaps forced by the sun, that influence the probability of a regime-shifting event. If it is possible to detect ''critical slowing down'' prior to the onset of the GIs, then this would serve as evidence that there are such slow variations in system stability and that these changes are important components in the dynamics of the DO cycles. Thus, the hypothesis is as follows: in the stadial periods of the last glaciation, there were slow changes to dynamical processes operating on decadal time scales, and these changes were associated with a weakening of the stability of the stadial climate states in Greenland and thereby increased the probability of the onset of interstadials.

An equilibrium climate state is stable if the system will return to this state subsequent to a small perturbation. If the state is weakly stable, then the effect of a perturbation will be larger and more long lasting than it would be if the equilibrium state is strongly stable. Hence, if an equilibrium climate state experiences reduced stability, the effects of random perturbations will grow in amplitude and become more persistent.

Within a dynamical systems framework, these questions can be discussed in terms of the stability of fixed points, and one can use a very simple scalar model to illustrate the effect of stability weakening:

$$dx(t) = F[x(t)]\,dt + \sigma\,dB(t). \tag{1}$$

Here x can be thought of as the climate variable we seek to model (e.g., the δ^{18}O ratio[2]), $dB(t)$ is a white noise forcing of the system, and $F(x) = -U'(x)$ is a nonlinear function corresponding to a potential $U(x)$. An example of such a model is shown in Fig. 1 The system has two stable fixed points, x_s and $x_{\rm is}$, corresponding to the stadial and interstadial states. These two stable states are separated by a potential barrier with an unstable fixed point. If the noise term $\sigma dB(t)$ is sufficiently strong compared to the potential barrier, there is a non-negligible probability of a spontaneous transition between the two stable states. Such transitions are completely noise induced.

On the other hand, we can also have a transition from the state x_s to the state $x_{\rm is}$, even in the absence of any noise, if the system goes through a bifurcation point. This means that the system depends on a slowly changing parameter r in such a way that x_s becomes unstable when a critical parameter value r_c is attained—that is, $F'_r(x_s) \to 0$ as $r \to r_c$. The dotted line in Fig. 1a shows how the stable fixed point x_s is lost under a so-called fold bifurcation. The linearization of Eq. (1) around x_s,

$$dx(t) = -\theta[x(t) - x_s]\,dt + \sigma dB(t), \tag{2}$$

is known as the Langevin stochastic differential equation, and its solutions define a stochastic process called the Ornstein–Uhlenbeck (OU) process, which in discrete time is a first-order autoregressive [AR(1)] process. The standard deviation of $x(t)$ in an OU process is $\sigma(2\theta)^{-0.5}$ and the autocorrelation is $e^{-\theta t}$. Since

[2] This time series is shown in Fig. 3.

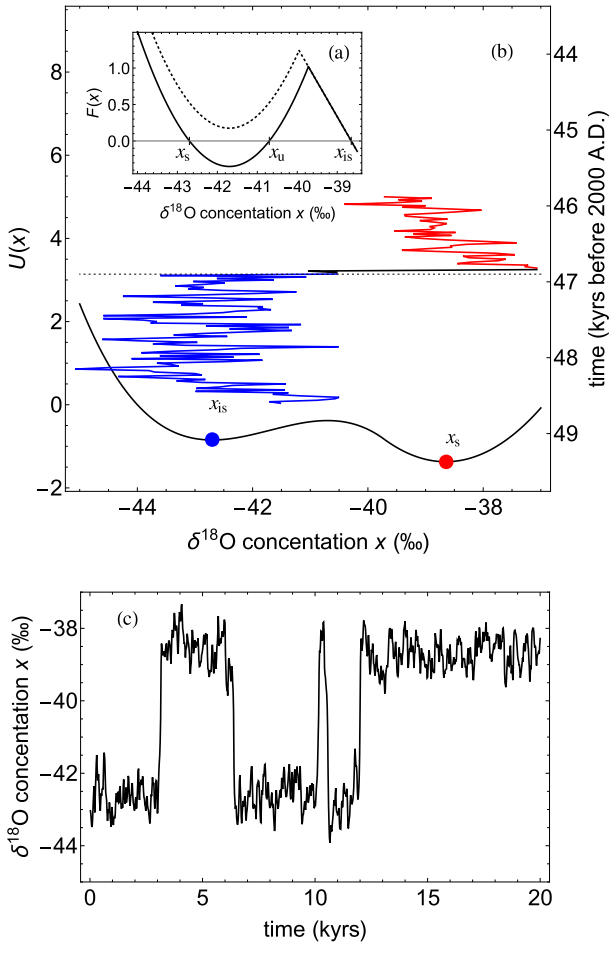

FIG. 1. (a) The function $F(x)$ in the example model. The dotted line shows $F(x)$ after a fold bifurcation. (b) The corresponding potential $U(x)$. The blue curve is the δ^{18}O signal prior to the onset of GI-12, and the red curve is the δ^{18}O signal during GI-12. (c) A realization of the model in Eq. (1) with $F(x)$ as shown (as the solid line) in (a).

$\theta = -F_r'(x_s)$, we expect increased fluctuation levels and longer correlation times of the signal $x(t)$ as the bifurcation approaches. These signatures are called early-warning signals (EWS) of the tipping point, or critical slowing down (Lenton et al. 2012; Dakos et al. 2008).

There is a key difference between a bifurcation in a completely deterministic low-dimensional dynamical system and a tipping point in a randomly forced system, since in the latter we need not actually reach a bifurcation point in order to see a shift between two stable states. All tipping points in randomly driven systems are to some extent noise induced, and the interesting question is whether the random fluctuations are sufficient to cause a shift between the two states or whether we can observe slow changes (perhaps forced) in the stability of the climate state. Even if EWS are not prominent features in the temperature records, observation of such structural changes may provide important insight into the mechanisms of climate tipping points.

A few authors have already attempted to identify EWS for DO events. Ditlevsen and Johnsen (2010) have demonstrated that it is very difficult to observe any such signatures in the Greenland ice-core data and that the ice-core data are inconsistent with what we observe in typical tipping point models. On the other hand, Cimatoribus et al. (2013) have suggested using the repeated DO events to construct an ensemble analysis that could uncover EWS that are not easily observable in the individual events. However, one must be very careful with how these ensembles are constructed. If we wish to look for EWS to the onsets of the interstadial warm periods, then the time intervals of interest are the stadial periods preceding these events. If the ensembles are constructed in such a way that the rapid cooling that marks the beginning of a stadial period is included in the ensemble members, then because of the particular timing of DO events, one is led to the false conclusion that the fluctuation levels increase significantly as the onset of an interstadial period is approaching. On the other hand, if the ensemble is constructed in such a way that only stadial periods (defined as the cold periods following the rapid cooling that mark the end of the interstadials) are included, then no significant EWS is seen in a standard analysis.

It appears that these results support the findings of Ditlevsen and Johnsen (2010), but perhaps one cannot expect to see EWS without analyzing individual frequency bands separately. In section 2, it will be shown that there are anomalous fluctuation levels on decadal time scales in the NGRIP data and that this is an indication that one should focus on these time scales when looking for EWS. In section 3, the NGRIP data are filtered to remove low-frequency variability, and then there is a slow increase in the fluctuation levels as the onsets of the interstadial periods are approached. This result is obtained by averaging over the sequence of events to obtain statistical significance, using the continuous wavelet transform (CWT):

$$W(t,\Delta t) = \frac{1}{\sqrt{\Delta t}} \int x(t')\psi\left(\frac{t-t'}{\Delta t}\right) dt', \qquad (3)$$

where $\psi(t)$ is the so-called mother wavelet. The CWT measures the fluctuations in the NGRIP signal $x(t)$ at various different time scales Δt and is hence a useful tool for discerning changes in the statistical properties of the signal in specific frequency bands.

The local high-frequency fluctuation levels are computed by taking the standard deviation of the wavelet

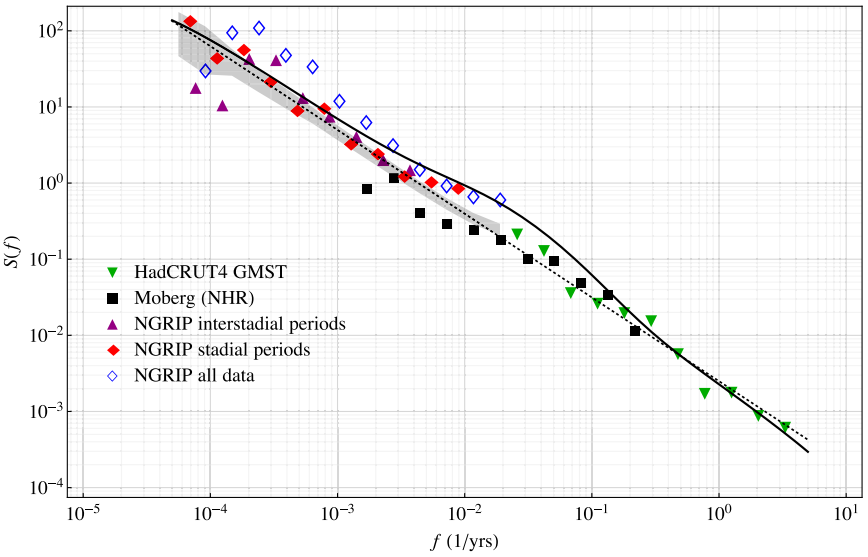

FIG. 2. Double-logarithmic plots of the PSD $S(f)$. The analysis of the 20-yr mean NGRIP data is shown as the blue diamonds, the purple triangles, and the red diamonds. The blue diamonds show the results of the analysis of the entire dataset dating back to 60 kyr BP. The red diamonds are the results of the analysis performed on the stadial periods only, and the purple triangles are the results of the analysis of the interstadial periods only. For comparison, the green triangles represent the HadCRUT4 monthly global mean surface temperatures and the black squares are the analysis of the Moberg Northern Hemisphere temperature reconstruction. (The PSDs of the NGRIP data have been shifted to make it easier to compare with the PSDs of the two other datasets.) The black curve is obtained from the expression in Eq. (4) (with $\beta = 1.15$) by increasing the parameters τ_k corresponding to time scales between a decade and a century. The shaded area represents the confidence region (in this case taken as two standard deviations) of the PSD estimate for a $1/f^{\beta}$ noise with 3000 data points (as in the NGRIP record).

coefficients corresponding to the short time scales Δt, and the time evolution of these are analyzed. For several of the events a significant increase in the standard deviations through the stadial periods is observed. Similar results are obtained for the wavelet estimates of the local Hurst exponent, implying that the characteristic correlation time in the high-frequency band increases as the onset of an interstadial is approached. The motivation for using Hurst exponents is explained toward the end of section 2, and the details of the wavelet-based analysis are presented in section 3. To optimize the time resolution a Paul mother wavelet is used in estimating the high-frequency fluctuation levels. For the estimation of the local Hurst exponent the scale resolution is important, and therefore the best choice is to use the Morlet mother wavelet (De Moortel et al. 2004).

2. Anomalies with respect to the $1/f^{\beta}$ climate noise

In this section it is shown that during the stadial periods of the NGRIP record there are deviations from the so-called $1/f$ law for temporal temperature variability. The anomaly is observed for the high frequencies, and this is consistent with the hypothesis that there are instabilities related to dynamical processes operating on decadal time scales. This will serve as a motivation for focusing specifically on the high-frequency band of the NGRIP record when analyzing critical slowing down.

Evidence of reduced stability on the decadal time scales during the last ice age can be observed in the estimated power spectral density (PSD) function of ice-core temperature proxies. In Rypdal and Rypdal (2016) it is shown that if the stadial and interstadial periods in the NGRIP data are analyzed separately, then fluctuations scale approximately as a $1/f$ noise, meaning that the PSD has the form $S(f) \sim f^{-\beta}$, with $\beta \approx 1$. The $1/f$ scaling observed in ice-core temperature variability is similar to what is observed in other temperature records, such as the instrumental global surface temperature and the Northern Hemisphere temperature reconstructions for the last two millennia (Rypdal and Rypdal 2016). In fact, the $(1/f^{\beta})$-type climate noise is what is typically observed for both global temperatures and for local temperatures, and deviations from this property can be seen as anomalous. One well-known example is El Niño–Southern Oscillation (ENSO), which places larger fluctuation levels on

the time scales of a few years than what is expected from a $1/f^{\beta}$ law (Løvsletten and Rypdal 2016). Another example is the large temperature variability on the decadal time scales observed in the Greenland ice cores. It must be noted that in the instrumental temperature records it is found that local land temperatures scale with a lower β exponent compared to global surface temperature and local sea surface temperatures (Rypdal et al. 2015; Løvsletten and Rypdal 2016; Fredriksen and Rypdal 2016), but on sufficiently long time scales we expect local and global temperatures to scale with the same exponent (Rypdal and Rypdal 2016). Figure 2 shows the estimated PSD of the δ^{18}O variations in the NGRIP ice core. The blue diamonds are the periodogram estimate for the entire time series, whereas the red diamonds and the purple triangles are estimated using only the stadial and interstadial periods separately. This can be done using the Lomb–Scargle periodogram (Lomb 1976), which is an estimation technique for the PSD that does not require the signal to be sampled at equal time intervals. As we see from the figure, the PSD deviates from the $1/f^{\beta}$ law for frequencies corresponding to time scales shorter than a few centuries. This effect can be taken as an indication that the processes that dominate the temperature signal on these time scales have weaker stability than what is predicted from a $1/f^{\beta}$ assumption. The argument behind this claim is that the scaling of the climate noise is a reflection of the fact that the climate system consists of many components that respond to perturbations on different time scales, and it is difficult to identify any characteristic time scales in the temperature records. As a simple explanatory model, we can think of the temperature signal as an aggregation of processes:

$$T(t) = \sum_k T_k(t),$$

where each term $T_k(t)$ is a (possibly) nonlinear and stochastic description of the temperature variations at the time scale τ_k. As linearized descriptions of the components $T_k(t)$ we can write the stochastic differential equations:

$$dT_k(t) + \theta_k T_k(t)\, dt = c_k dB_k(t), \quad \text{with} \quad \theta_k = \frac{1}{\tau_k},$$

and from this (assuming independence if the noise processes dB_k) the PSD of the aggregated signal $T(t)$ becomes

$$S(f) = \sum_k \frac{|c_k|^2}{\tau_k^{-2} + (2\pi f)^2}. \tag{4}$$

The aggregated process $T(t)$ can be made to approximate a $1/f^{\beta}$ noise if we choose the time scales τ_k to be exponentially spaced (i.e., $\tau_k = a^k \tau_0$ for some parameter $a > 0$). Here τ_0 is some reference time scale (e.g., $\tau_0 =$ 1 yr). In addition we need to require that $|c_k|^2 = a^{2-\beta}|c_{k+1}|^2$. If this is the case we have the approximate relation $S(af) \approx a^{-\beta} S(f)$, so if $\beta \approx 1$ the signal $T(t)$ will be consistent with the scaling observed in ice-core temperature records.

This model is clearly constructed to produce the $(1/f^{\beta})$-type scaling observed in temperature records. However, the superposition of OU processes can be motivated by simple physical considerations. One way is to use a very simple N-box model for the vertical heat transport in the oceans. In such a model, which is a straightforward generalization of the two-box model introduced by Held et al. (2010), it can be shown that the surface temperature is a convolution on the following form:

$$T(t) = \int_t \left[\sum_{k=1}^{N} c_k e^{-\theta_k (t-s)} \right] dF(s),$$

where the parameters c_k and the system eigenvalues $\theta_k > 0$ depend on the heat conductivities and the heat capacities of the boxes. If the forcing $F(t)$ is taken to be a white-noise process—that is, $dF(t) = dB(t)$—then the temperature is a linear combination of dependent OU processes, and if we have a clear separation of scales so that each characteristic times scale $\tau_k = \theta_k^{-1}$ is much longer than the correlation time $\tau_{k-1} = \theta_{k-1}^{-1}$ of the subsequently faster mode, then the cross covariance between the processes is small and the expression in Eq. (4) is a good approximation of the PSD.

Using this description we can now explore the effect of reducing the stability of some of the components T_k. For instance, if one of the components $T_k(k)$ is well described by a nonlinear model that approaches a tipping point, then in the linearized model we will see $\theta_k \to 0$, corresponding to a strong increase in the characteristic time scale τ_k. This will lead to a deviation from the (approximate) $1/f^{\beta}$ law. In fact, this effect is completely consistent with our observations for the NGRIP data. The black curve in Fig. 2 is obtained from the expression in Eq. (4) (with $\beta = 1.15$) by increasing the parameters τ_k corresponding to time scales between a decade and a century (using $a = 2$ and $\tau_0 = 1$ yr). The effect is a "flattening" of the PSD on time scales shorter than a few centuries, similar to what is estimated in the NGRIP data.

From Fig. 2 one can also observe that if the entire NGRIP record is analyzed (the blue diamonds), then there is an apparent "scale break," with $1/f^{\beta}$ and $\beta \approx 1$, for the frequencies corresponding to time scales longer than about 500 yr. The increased β value is actually not a characterization of the variability in the stadial or interstadial states but an effect of the shifts between the

two states. What is relevant for this paper is the scaling under stadial conditions (the red diamonds). This is close to a $1/f$ noise except for the high-frequency band. A detailed analysis of the scaling properties in the NGRIP data is given in Rypdal and Rypdal (2016).

In Rypdal and Rypdal (2016) the scaling analysis is also carried out using a wavelet-based approach. If the PSD is a power law—that is, $S(f) \sim f^{-\beta}$—then the variance of the wavelet transforms scales according to $\langle W(t, \Delta t)^2 \rangle \sim \Delta t^{\beta}$, as a function of the time scale Δt. A white-noise process corresponds to $\beta = 0$ and a Brownian motion has $\beta = 2$. An OU process, which has a Lorentzian PSD, will have a scaling regime $\beta = 0$ for time scales much larger than the correlation time and a scaling regime $\beta = 2$ on time scales much shorter than the correlation time. A common definition of the Hurst exponent is $H = (\beta + 1)/2$, and for a stationary (zero mean) process with $\beta < 1$ the temporal correlations in the signal are related to the Hurst exponent via the following formula:

$$\langle x(t)x(t + \Delta t)\rangle \sim 2H(2H - 1)\Delta t^{2H-2}.$$

For $\beta > 0$ the covariance is not well defined, but a similar formula can be written for the increment process. If the signal is not scaling, it is still possible to estimate a local Hurst exponent by interpreting the relation $\langle W(t, \Delta t)^2 \rangle \sim \Delta t^{\beta}$ as the high-frequency limit $\Delta t \to 0$, similar to how one defines a fractal dimension. In this case the Hurst exponent does not quantify the autocorrelation decay of the signal $x(t)$ but rather the roughness of the signal. It can also be taken as a measurement of the correlation decay for the high-frequency component for the signal. Note that an OU process has $H = 1.5$ ($\beta = 2$) in the high-frequency limit, so if the signal $x(t)$ is the superposition of OU processes with distinct characteristic time scales τ_k and the PSD of the aggregated signal is a $1/f^{\beta}$ law with $\beta \approx 1$, then the locally estimated Hurst exponent will increase toward $H = 1.5$ if the signal is modified so that the terms corresponding to short correlation times τ_k become more dominant. A thorough account of wavelet-based techniques and Hurst analysis for scaling processes is given by Malamud and Turcotte (1999).

The main conclusion of this section is that there is a deviation from the $1/f^{\beta}$ law for high frequencies during the stadial periods in the NGRIP record. This observation indicates that the high-frequency fluctuations in the NGRIP data are of interest when searching for EWS, but in itself this observation does not present any EWS, since it does not uncover any temporal changes in the stability of the stadial climate state. Such changes will be discussed in the next section.

3. Analysis and results

As discussed in the introduction, if one attempts to model the NGRIP δ^{18}O times series as a single randomly forced scalar dynamical system with two stable states, then any parameter choice that corresponds to realistic fluctuation levels in the stadial and interstadial states will lead to spontaneous "jumps" between the two states. This is a simple consequence of the ratios between the fluctuation level and the temperature difference between the stadial and interstadial states. This is illustrated in Fig. 1, which shows an example of such a model. Here the parameters are chosen so that the OU models (which are obtained by linearization around the stadial and interstadial states) have standard deviations equal to the sample standard deviations of the stadial and interstadial periods in the NGRIP time series. The fixed points are chosen according to the averages of δ^{18}O in the stadial and interstadial periods before and after the onset GI-12.[3] Figure 1c shows a realization of this model with fixed parameters, and it is observed that there are transitions between the two states even in the absence of any slowly varying parameter changes (i.e., completely noise-induced shifts). For a model of this kind, the onset times of the GIs would have no periodic component.

However, as discussed in section 2, it is reasonable to model the δ^{18}O signal as an aggregation of signals. It is then possible that the shifts do require reduced stability of the stadial climate state. If this is the case, we should in principle observe EWS, but these may be masked by low-frequency variability. A natural approach for uncovering EWS is then to filter the NGRIP data and analyze certain frequency bands. As also discussed in section 2, there are indications that the dynamical processes associated with reduced stability have characteristic time scales shorter than a century, suggesting analysis of the high-frequency band of the NGRIP data.

The first step of this analysis is to identify stadial periods and the onset times for the interstadial periods. In total 18 climate events are analyzed. These include the onsets of GIs 1–17 as well as the YD–Preboreal transition, using the onset dates for the interstadial periods (and the date for the YD–Preboreal transition) as given by Svensson et al. (2008). These dates determine the end of the cold periods that are investigated for EWS. The start dates for the cold periods are chosen such that they do not include the very sudden temperature declines that often occur in the DO cycles. These sudden temperature changes (which are believed to be linked to

[3] We refer to Svensson et al. (2008) for the enumeration of the GIs.

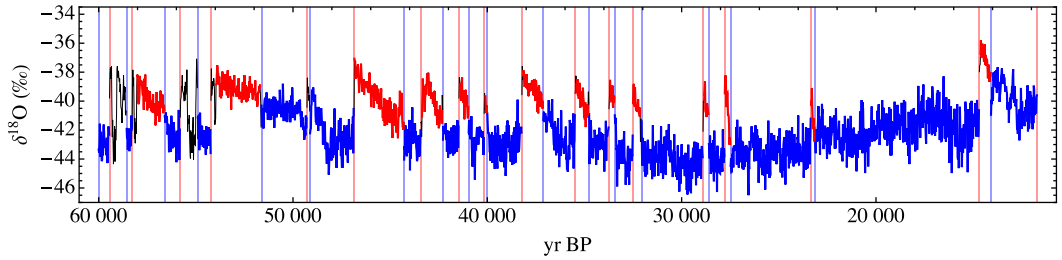

FIG. 3. The NGRIP δ^{18}O record. The parts of the curve that are drawn in blue are defined as the cold periods, and it is these data that are analyzed for EWS. The parts of the curve that are drawn in red are defined as the warm periods, and these are used to compute the PSD for the interstadial periods that is shown in Fig. 2.

slowdowns of the thermohaline circulation coupled with sea ice formation) can themselves be seen as tipping points (Lenton et al. 2012) and should not be viewed as a part of the destabilization of the cold state. The cold periods we have chosen to analyze are drawn as blue curves in Fig. 3.

Figure 4 shows the results of an analysis where each cold period is considered as an ensemble member. The δ^{18}O time series is filtered by subtracting a 100-yr moving average, and for the filtered signal the standard deviation is computed in running 100-yr windows. For the cold periods (those drawn in blue in Fig. 3), the results are organized by averaging the standard deviation over all 100-yr time windows that precede the onset of an interstadial period by a certain number of years. This yields an ensemble estimate of the fluctuation level in the δ^{18}O signal as a function of the time before the sudden onset of the warm period. Figure 4b shows the fluctuation level when all cold periods (except the YD) with duration longer than 300 yr are included. The dotted line is a linear fit with a slope $\hat{a}_\sigma = 0.08‰\,\mathrm{kyr}^{-1}$.

This increasing slope is significantly larger than zero, with a p value of 0.04. The significance is tested by constructing signals that have the same PSD as the cold-period signals but where the phases are randomized. For each of the cold periods the discrete Fourier transform (DFT) of the δ^{18}O signal is computed, and for each frequency the square root of its modulus is multiplied by a factor $e^{i\phi}$, where ϕ is a random angle chosen with respect to the uniform distribution on the interval $[0, 2\pi)$. The inverse DFT is applied to the resulting time series, before taking the real parts and adjusting the standard deviations by a factor $\sqrt{2}$.[4] The thin curves in Fig. 4b show how the standard deviations in 100-yr windows of the (filtered) synthetic realizations depend on the time before the onset of the interstadial periods. In a large ensemble of realizations the pseudoslopes $\hat{a}_\sigma$ are computed, and the distribution function $P(\hat{a}_\sigma)$ of these is obtained using a smooth kernel estimator (Rosenblatt 1956). The estimated distribution function is shown in Fig. 4d. The arrow in this figure shows the value $\hat{a}_\sigma = 0.08‰\,\mathrm{kyr}^{-1}$ estimated from the δ^{18}O signal, and the gray area under the curve marks the 95% confidence interval for $\hat{a}_\sigma$ under the null model. The p value is computed as $p = 1 - P(0.08‰\,\mathrm{kyr}^{-1})$. Figures 4a,c show the results of the same analysis, but in this case the YD–Preboreal transition is included in the analysis, which in practice means that the YD is included as one of the cold periods under investigation. When the YD is included the estimate becomes $\hat{a}_\sigma = 0.11‰\,\mathrm{kyr}^{-1}$, whereas the distribution $P(\hat{a}_\sigma)$ changes very little, and the statistical significance is improved to $p = 0.005$.

The results presented above show that if we view the sequence of DO events as a statistical ensemble, there is on average a tendency for the fluctuation levels to increase toward the sudden termination of the Greenland stadials. However, it does not tell us whether these EWS are observable in the individual climate events. The individual events are analyzed using the CWT defined in Eq. (3), and the local high-frequency fluctuation levels are computed by taking the standard deviation of the wavelet coefficients corresponding to the short time scales. Then the time evolution of these are analyzed; that is, the wavelet coefficients are averaged over the time scales $0 < \tau < \tau_c$ and over time windows of length Δt:

$$\sigma^2(t) = \frac{1}{\Delta t}\int_0^{\tau_c}\int_{t-\Delta t/2}^{t+\Delta t/2} |W(t',\tau)|^2\, dt'\, d\tau. \qquad (5)$$

I have used $\tau_c = 50$ yr and $\Delta t = 200$ yr, and the time variation of $\sigma(t)$ for each cold period is shown in Fig. 5a. Linear fits to $\sigma(t)$ in each cold period are drawn in red, and realizations of $\sigma(t)$ for the synthetic signals (using the same null model as described above) are plotted as the thin curves. The distribution function for the linear pseudotrends in the null model is obtained via a smooth kernel estimator, and using this p values for the linear increases in $\sigma(t)$ are computed. These p values are shown in Fig. 5a. We have $p < 10^{-4}$ prior to the onset of the

[4] Since we disregard the imaginary part of the constructed signal, this adjustment is needed in order for the synthetic signals to have the same standard deviations as the cold periods in the δ^{18}O signal.

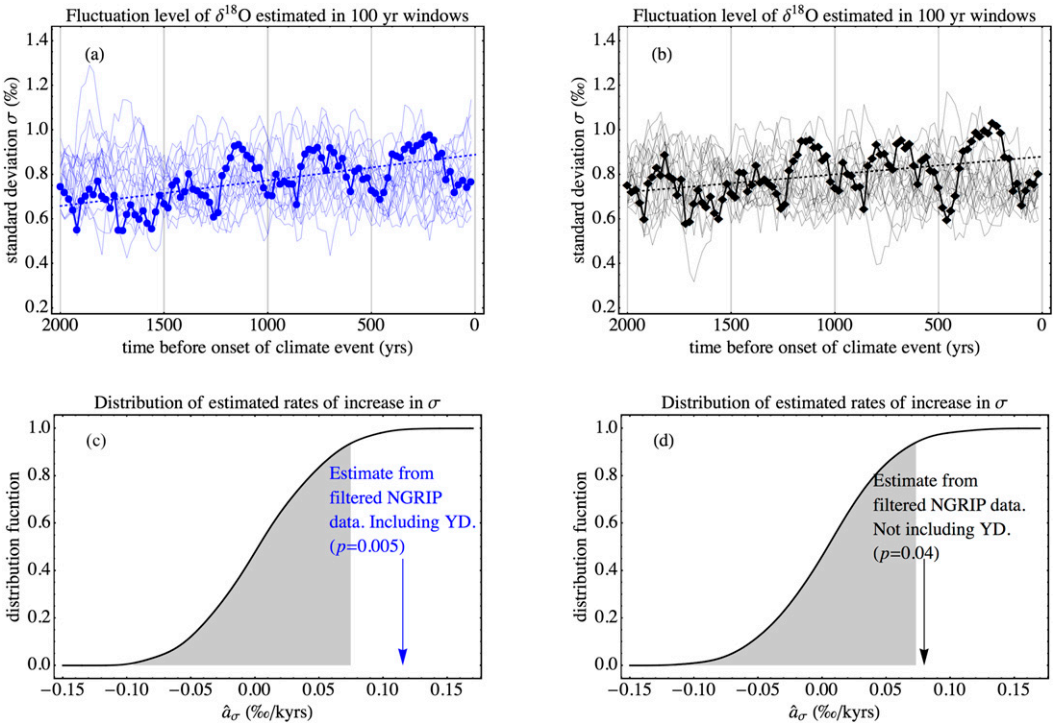

FIG. 4. (a) The fluctuation level in 100-yr windows of the filtered δ^{18}O signal as a function of the time before the sudden onset of the warm period. The dotted line is a linear fit $\hat{a}_\sigma = 0.11‰\,\text{kyr}^{-1}$. The thin curves are the corresponding fluctuation levels in a null model, which is constructed by taking the PSD of each cold period and randomizing the phases. (b) As in (a), but in this case the YD is not included as one of the cold periods. The dotted line has the slope $\hat{a}_\sigma = 0.07‰\,\text{kyr}^{-1}$. (c) The distribution function of the linear fits $\hat{a}_\sigma$ under the null model. The shaded area represents the 95% confidence of $\hat{a}_\sigma$ under the null model and the arrow marks the observation $\hat{a}_\sigma = 0.11‰\,\text{kyr}^{-1}$. (d) As in (c), but in this case for the analysis that does not include the YD. The arrow marks the estimate $\hat{a}_\sigma = 0.08‰\,\text{kyr}^{-1}$.

YD–Preboreal transition and prior to the onsets of GI-1 and GI-8. Prior to GI-12 we have significance at the 0.1 level, and in a majority of the cold periods we have increasing trends in $\sigma(t)$. From Fig. 5a one can also observe that the fluctuation level during the YD is higher than for the preceding stadial periods in the NGRIP record, and in Fig. 3 one observes that this period is significantly warmer compared to most of the other stadial periods. These are climate conditions closer to what is experienced in the Holocene, and indeed, the YD period can be viewed as a part of the termination of the ice age.

Figure 4b shows the time dependence of the locally estimated Hurst exponent H. This is estimated via the following relation:

$$\langle |W(t,\tau)|^2 \rangle \sim \tau^{2H-1};$$

that is, a linear fit is made to $\log\langle |W(t,\tau|^2\rangle$ as a function of $\log\,\tau$. The fluctuations $\langle |W(t,\tau|^2\rangle$ are estimated in 200-yr windows and only the time scales shorter than 60 yr are used. Since only the high-frequency fluctuations are used to estimate H it is more appropriate to think of it as a local smoothness exponent than as a scaling exponent. Nevertheless, a time-varying Hurst exponent estimate that increases in time is consistent with an increase in correlation time in the high-frequency band, and it is thus expected in association with stability loss. As with the high-frequency wavelet fluctuation level, there are strongly significant increases in H before the onsets of GI-1 and the YD–Preboreal transition. Strong increases are also seen before GI-8 and GI-4.

4. Discussion and concluding remarks

This paper presents both new results and new methods. The new methods include combining high-pass filtering with the ensemble construction presented by Cimatoribus et al. (2013), as well as using the wavelet transform to discern time-varying fluctuations in the high-frequency band. Another important aspect is the statistical significance testing, which is based on a nonparametric null model with random phases. Because of the "flattening" of the PSD at high frequencies, the application of a parametric model such as a fractional Gaussian noise (fGn) will lead to a misrepresentation of the fluctuation levels either on the short time scales or on the long time scales

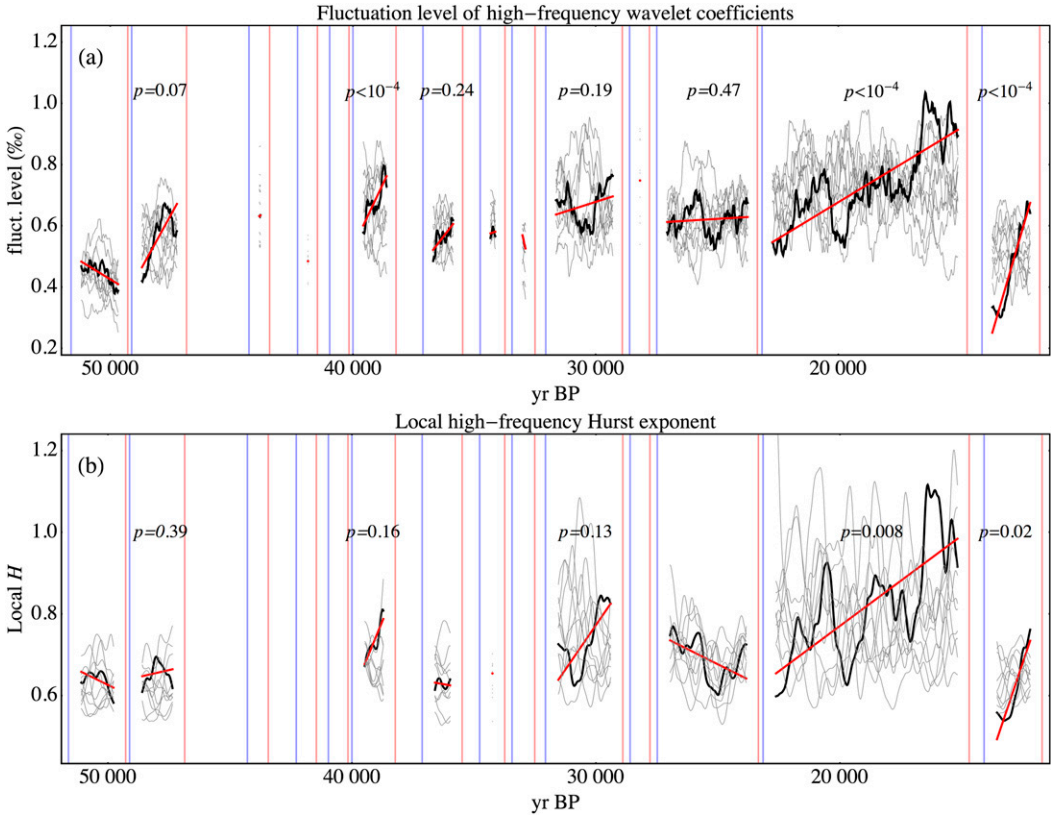

FIG. 5. (a) The wavelet fluctuation level $\sigma(t)$ defined by Eq. (5). The red curves are linear fits to $\sigma(t)$ in each cold period, and the p values are obtained by estimating the distribution function for the linear slopes using a Monte Carlo simulation (with the null model that is constructed by randomizing the phases). (b) As in (a), but for the locally estimated Hurst exponent.

(depending on which time scales are emphasized in the parameter estimation). In either case it will provide an inaccurate model for the distribution of pseudotrends in the local fluctuation levels. For instance, if one were to apply an fGn null model using standard parameter estimation methods, then this model would underestimate the high-frequency fluctuation levels, and as a consequence one would obtain much lower p values for the EWS.

The methods described above are different from those used by Lenton et al. (2012) and Dakos et al. (2008), who focus on the lag-1 autocorrelation and the Hurst exponent estimated using detrended fluctuation analysis (DFA). While these approaches are very robust, they have some disadvantages. A problem with the lag-1 autocorrelation is its sensitivity to trends and to low-frequency variability that is not easily removed by standard detrending methods, and the DFA estimator is known to resolve time scales poorly. The filtering applied in Lenton et al. (2012) and Dakos et al. (2008) is meant as a detrending, and care is made not to filter out the low-frequency variability in the signal, while in this paper it is a point to remove the slow fluctuations that are masking the EWS.

The EWS we find for the YD–Preboreal transition are consistent with results of Lenton et al. (2012) and Dakos et al. (2008). We also find strong EWS for the onset of GI-1 (the so-called Bølling–Allerød warming) and GI-8, and seen as an ensemble, we find significant EWS for the onsets of the interstadial periods. The results show that there are dynamical structures related to some of the DO cycles that experience reduced stability prior to the onset of a sudden warming. This is in contradiction to Ditlevsen and Ditlevsen (2009) and Ditlevsen and Johnsen (2010), who conclude that the onsets of GIs must be seen as random and unpredictable events. However, even though it is demonstrated that there are EWS for the onsets of the GIs, it is also recognized that these are difficult to observe in the climate noise and that it is necessary to filter out the low-frequency fluctuations in order to obtain statistically significant results. This implies that any probabilistic prediction method of DO events based on the EWS will have low sharpness, and in this sense, the results of this study only partly contradict the main message of Ditlevsen and Johnsen (2010).

The observation that the stadial climate in Greenland experiences reduced stability prior to the onsets of the interstadials is complementary to the findings of Livina et al. (2010), who have made similar observations (using very different methods) for the interstadial climate states. The study of Livina et al. (2010) is consistent with the observation of EWS in climate models forced through a shutdown of the Atlantic thermohaline circulation (Lenton et al. 2012).

Acknowledgments. This work has received support from the Norwegian Research Council under Contract 229754/E10. The author thanks K. Rypdal, H.-B. Fredriksen, T. Nilsen, and O. Løvlsetten for useful discussions and suggestions.

REFERENCES

Balenzuela, P., H. Braum, and D. R. Chialvo, 2012: The ghost of stochastic resonance: An introductory review. *Contemp. Phys.*, **53**, 17–38, doi:10.1080/00107514.2011.639605.

Bond, G. C., W. Showers, M. Elliot, M. Evans, R. Lotti, I. Hajdas, G. Bonani, and S. Johnson, 2013: The North Atlantic's 1-2 Kyr climate rhythm: Relation to Heinrich events, Dansgaard/Oeschger cycles and the Little Ice Age. *Mechanisms of Global Climate Change at Millennial Time Scales*, *Geophys. Monogr.*, Vol. 112, Amer. Geophys. Union, 35–58.

Braun, H., M. Christl, S. Rahmstorf, A. Ganopolski, A. Mangini, C. Kubatzki, K. Roth, and B. Kromer, 2005: Possible solar origin of the 1,470-year glacial climate cycle demonstrated in a coupled model. *Nature*, **438**, 208–211, doi:10.1038/nature04121.

Broecker, W. S., G. H. Denton, R. L. Edwards, H. Cheng, R. B. Alley, and A. E. Putnam, 2010: Putting the Younger Dryas cold event into context. *Quat. Sci. Rev.*, **29**, 1078–1081, doi:10.1016/j.quascirev.2010.02.019.

Cimatoribus, A. A., S. S. Drijfhout, V. Livina, and G. van der Schrier, 2013: Dansgaard–Oeschger events: Bifurcation points in the climate system. *Climate Past*, **9**, 323–333, doi:10.5194/cp-9-323-2013.

Curry, J., J. L. Schramm, and E. E. Ebert, 1995: Sea ice–albedo climate feedback mechanism. *J. Climate*, **8**, 240–247, doi:10.1175/1520-0442(1995)008<0240:SIACFM>2.0.CO;2.

Dakos, V., M. Scheffer, E. H. van Nes, V. Brovkin, V. Petoukhov, and H. Held, 2008: Slowing down as an early warning signal for abrupt climate change. *Proc. Natl. Acad. Sci. USA*, **105**, 14 308–14 312, doi:10.1073/pnas.0802430105.

Dansgaard, W., S. J. Johnsen, H. B. Clausen, D. Dahl-Jensen, N. Gundestrup, C. U. Hammer, and H. Oeschger, 1984: North Atlantic climatic oscillations revealed by deep Greenland ice cores. *Climate Processes and Climate Sensitivity*, *Geophys. Monogr.*, Vol. 29, Amer. Geophys. Union, 288–298.

——, and Coauthors, 1993: Evidence for general instability of past climate from a 250-kyr ice-core record. *Nature*, **364**, 218–220, doi:10.1038/364218a0.

De Moortel, I., S. A. Munday, and A. W. Hood, 2004: Wavelet analysis: The effect of varying basic wavelet parameters. *Sol. Phys.*, **222**, 203–228, doi:10.1023/B:SOLA.0000043578.01201.2d.

Ditlevsen, P. D., and O. D. Ditlevsen, 2009: On the stochastic nature of the rapid climate shifts during the Last Ice Age. *J. Climate*, **22**, 446–457, doi:10.1175/2008JCLI2430.1.

——, and S. J. Johnsen, 2010: Tipping points: Early warning and wishful thinking. *Geophys. Res. Lett.*, **37**, L19703, doi:10.1029/2010GL044486.

——, K. K. Andersen, and A. Svensson, 2007: The DO-climate events are probably noise induced: Statistical investigation of the claimed 1470 years cycle. *Climate Past*, **3**, 129–134, doi:10.5194/cp-3-129-2007.

Fredriksen, H.-B., and K. Rypdal, 2016: Spectral characteristics of instrumental and climate model surface temperatures. *J. Climate*, **29**, 1253–1268, doi:10.1175/JCLI-D-15-0457.1.

Grootes, P. M., and M. Stuiver, 1997: Oxygen 18/16 variability in Greenland snow and ice with 10^{-3}- to 10^{5}-year time resolution. *J. Geophys. Res.*, **102**, 26 455–26 470, doi:10.1029/97JC00880.

Held, I. M., M. Winton, K. Takahashi, T. Delworth, F. Zeng, and G. K. Vallis, 2010: Probing the fast and slow components of global warming by returning abruptly to preindustrial forcing. *J. Climate*, **23**, 2418–2427, doi:10.1175/2009JCLI3466.1.

Lenton, T. M., V. N. Livina, V. Dakos, E. H. van Nes, and M. Scheffer, 2012: Early warning of climate tipping points from critical slowing down: Comparing methods to improve robustness. *Philos. Trans. Roy. Soc. London*, **370A**, 1185–1204, doi:10.1098/rsta.2011.0304.

Li, C., D. S. Brattisi, and C. M. Blitz, 2010: Can North Atlantic sea ice anomalies account for Dansgaard–Oeschger climate signals? *J. Climate*, **23**, 5457–5475, doi:10.1175/2010JCLI3409.1.

Livina, V. N., F. Kwasniok, and T. M. Lenton, 2010: Potential analysis reveals changing number of climate states during the last 60 kyr. *Climate Past*, **6**, 77–82, doi:10.5194/cp-6-77-2010.

Lomb, N. R., 1976: Least-squares frequency analysis of unequally spaced data. *Astrophys. Space Sci.*, **39**, 447–462, doi:10.1007/BF00648343.

Løvsletten, O., and M. Rypdal, 2016: Statistics of regional surface temperatures post year 1900: Long-range versus short-range dependence and significance of warming trends. *J. Climate*, doi:10.1175/JCLI-D-15-0437.1, in press.

Malamud, B. D., and D. L. Turcotte, 1999: Self-affine time series: I. Generation and analyses. *Adv. Geophys.*, **40**, 1–90, doi:10.1016/S0065-2687(08)60293-9.

Manabe, S., and R. J. Stouffer, 1980: Sensitivity of a global climate model to an increase of CO_2 concentration in the atmosphere. *J. Geophys. Res.*, **85**, 5529–5554, doi:10.1029/JC085iC10p05529.

Rosenblatt, M., 1956: Remarks on some nonparametric estimates of a density function. *Ann. Math. Stat.*, **27**, 832–837, doi:10.1214/aoms/1177728190.

Rypdal, K., M. Rypdal, and H.-B. Fredriksen, 2015: Spatiotemporal long-range persistence in Earth's temperature field: Analysis of stochastic-diffusive energy balance models. *J. Climate*, **28**, 8379–8395, doi:10.1175/JCLI-D-15-0183.1.

Rypdal, M., and K. Rypdal, 2016: Late Quaternary temperature variability described as abrupt transitions on a 1/*f* noise background. *Earth Syst. Dyn.*, **7**, 281–293, doi:10.5194/esd-7-281-2016.

Sakai, K., and W. R. Peltier, 1999: A dynamical systems model of the Dansgaard–Oeschger oscillation and the origin of the bond cycle. *J. Climate*, **12**, 2238–2255, doi:10.1175/1520-0442(1999)012<2238:ADSMOT>2.0.CO;2.

Sonett, C. P., 1984: Very long solar periods and the radiocarbon record. *Rev. Geophys.*, **22**, 239–254, doi:10.1029/RG022i003p00239.

Suess, H. E., 2006: The radiocarbon record in tree rings of the last 8000 years. *Radiocarbon*, **22**, 200–209.

Svensson, A., and Coauthors, 2008: A 60 000 year Greenland stratigraphic ice core chronology. *Climate Past*, **4**, 47–57, doi:10.5194/cp-4-47-2008.